Cadmium and indium defects in ceria and their interaction with oxygen vacancies and small polarons

Alexandra K. A. Pryde, Shyam Vyas, and Robin W. Grimes*

The Royal Institution of Great Britain, 21 Albemarle Street, London W1X 4BS, United Kingdom

John A. Gardner and Ruiping Wang[†]

Department of Physics, Oregon State University, Corvallis, Oregon 97331-6507

Atomistic simulation calculations have been used to investigate the energetics of defect clustering and migration in ceria. The defects considered are In^{3+}, Cd^{2+}, their associated oxygen vacancies, and small polarons modeled as Ce^{3+} ions. Thus a range of complex defect clusters is considered. The overall aim of the study is to generate a better understanding of these defects as they relate to recent experimental results obtained using perturbed-angular-correlation spectroscopy. The calculations are successful in this regard, correctly predicting both binding energies and an oxygen migration activation energy. More importantly, the calculations provide an atomistic explanation for certain of the experimental observations. As such, the synergy between calculations and experiment is an important feature of this paper.

I. INTRODUCTION

Atomistic computer simulation techniques are presently being used to study point defects in a variety of materials. The Mott-Littleton method is one of the most widely applied.[1,2] It assumes an ionic description of the lattice, includes effective short-range pair potentials acting between ions and a shell model for polarizability. Within the model, defects are isolated and therefore relate, in the first instance, to an ideal solution limit. The information that the calculations can provide includes defect cluster binding energies, migration activation energies or structural data such as the extent of lattice relaxation around a defect center. In only a few cases however, can the data be compared directly with experiments that relate appropriately, to very small concentrations of defects which are disordered throughout the lattice. The present study is therefore significant since in the experimental work with which we wish to compare,[3-7] the concentration of In or Cd in the CeO_2 host lattice, is appropriately small. In addition, the hyperfine experiments were able to yield an unambiguous binding energy and also migration data all of which can be used to assess the reliability of the computer simulations. The close accord between experiment and theory strongly supports the subsequent use of the simulation results in providing the framework for understanding certain aspects of the experimental observations. The clear synergy between the computer model and experiment is an important aspect of this work.

In the first part of the paper we consider only those defect clusters that incorporate a single oxygen vacancy adjacent to a defective cation. In addition, the activation energies to move the position of the vacancy around the metal ion defects are described. These compare favorably with the experimental results.[3-7] Subsequently, we consider more complex defect clusters which may be formed from a combination of: multiple oxygen vacancies, more than one cation defect or small polaron Ce^{3+} ions. Such complexes

arise either as minority defects in ceria or are introduced by exploiting the potential range of nonstoichiometry that ceria can exhibit. Again, the aim of modeling more complex defect clusters is to provide data that will complement the hyperfine experiments of Gardner and co-workers.[3-7]

The relevant experimental studies,[3-7] conducted by Gardner and co-workers, used time-differential perturbed-angular-correlation spectroscopy (PAC) to study the behavior of oxygen vacancy defects adjacent to parent ^{111}In and daughter [111]Cd defect centers.

For these PAC studies, very dilute ($\sim 10^{-8}$) radioactive ^{111}In is introduced into the solution from which samples are made. The electromagnetic interaction with nearby lattice defects is measured through the perturbation of the angular distribution of γ rays emitted following decay of ^{111}In to [111]Cd.

When substituted for Ce in pure ceria, the PAC probe atom traps an electronic hole during the decay and their time-fluctuating interaction (so-called "aftereffects") causes the angular correlation to relax rapidly. For samples with modest oxygen vacancy concentrations, aftereffects are observed for some nuclei below 150 °C, but static electric-field-gradient interactions are observed for a substantial fraction of the nuclei. Clear PAC spectral frequencies can be associated with single oxygen vacancies at first-neighbor positions to the [111]Cd. The binding energy of vacancies to indium is large, but only the lower limit of order 0.35 eV can be determined from present experimental information.

Above 200 °C the PAC interaction is not static (on a time scale of 100 ns). The experimental data clearly indicate that the oxygen vacancies jump among first-neighbor trap sites over an energy barrier of 0.60 (2) eV.[7] For oxygen concentrations above approximately 0.05%, the PAC spectra indicate that significant fractions of the indium dopants are bound into clusters containing two or more oxygen vacancies.

TABLE I. Shell model parameters.

Ion	Y (e)	K (eV Å^{-2})
O^{2-}	-6.1	419.87
Ce^{4+}	7.7	291.75
Ce^{3+}	7.7	291.75
Cd^{2+}	-6.1	840.00
In^{3+}	-6.1	1680.00

TABLE II. Short-range potential parameters.

Interaction	A (eV)	ρ (Å)	C (eV Å^6)
O^{2-}-O^{2-}	22764.3	0.149	43.83
O^{2-}-Ce^{4+}	1986.83	0.35107	20.20
O^{2-}-Ce^{3+}	1731.62	0.36372	14.43
O^{2-}-Cd^{2+}	1725.99	0.3497	13.91
O^{2-}-In^{3+}	1795.65	0.3442	4.33

II. METHODOLOGY

A. Simulation technique

The procedures are based upon a description of the lattice in terms of effective potentials. The perfect lattice is described by defining a unit cell which is repeated throughout space using periodic boundary conditions as defined by the usual crystallographic lattice vectors. We consider interactions due to long-range Coulombic forces, which are summed using Ewald's method and also short-range forces that are modeled using parametrized pair potentials (as discussed below). Formal charge states are assumed on all ions (i.e., O^{2-}, Ce^{4+}, etc.). The short-range terms account for the electron cloud overlap and dispersion interactions which are negligible beyond a few lattice spacings. Thus, in order to reduce the computational time, the short-range interactions are set to zero beyond 8.66 Å. The total energy of the crystal is minimized by allowing the ions in the unit cell and the lattice vectors to relax to zero strain.

When calculating defect energies, the energy minimized perfect lattice is partitioned into two regions: a spherical inner region I at the center of which the defect is introduced and an outer region II which extends to infinity. In region I, interactions are calculated explicitly so that the response of the lattice to the defect is modeled by relaxing the positions of all ions to zero force using a Newton-Raphson minimization procedure. The response of region II is treated using the Mott-Littleton approximation.[1] In this study, the calculations were performed using the CASCADE code.[8]

To ensure a smooth transition between regions I and II, we incorporate an interfacial region IIa in which ion displacements are determined through the Mott-Littleton approximation but in which interactions with ions in region I are calculated by explicit summation. In the present calculations region I and region IIa radii were 10.82 and 20.02 Å, respectively. Region sizes were chosen to be large enough to ensure that no appreciable change in defect formation energy occurs if the region sizes are increased further.

All ions are treated as polarizable using the shell model.[9] In this, a massless shell of charge Y is allowed to move with respect to a massive core of charge X; the charge state of each ion is therefore equal to $(X+Y)$. The core and shell charges are connected by an isotropic harmonic spring of force constant k (see Table I). Displacement of the shell relative to the core gives a good description of electronic polarization.

B. Derivation of short-range parameters

The Buckingham potential form was chosen to represent the interaction energy $E(r)$ so that,

$$E(r) = A \exp\left(\frac{-r}{\rho}\right) - \frac{C}{r^6},$$

where A, r, and C are the variable parameters (see Table II). The host lattice potentials were taken from the work of Butler et al.[10] and have been used in a number of subsequent successful studies.[11,12] In this study, the Ce^{4+}-O^{2-} potential (the A potential) also incorporates a C_6 term which results in a superior fit to the CeO_2 experimental lattice parameter. The present potentials result in a calculated lattice parameter of 5.411 Å identical to the experimental value.[10] In addition, we find that the predicted dielectric constants, $\epsilon_0 = 19.51$ and $\epsilon_\infty = 4.0$ are in excellent agreement with the experimental values of $\epsilon_0 = 18.6$–20.0 and $\epsilon_\infty = 4.0$.[10]

The potentials that describe the interactions between the lattice and both the dopant Cd^{2+} and In^{3+} ions and the small polaron Ce^{3+} ion, were determined by an empiricizing procedure[10,13] which is described as follows. Dopant lattice interactions along with a trial Ce^{4+}-O^{2-} lattice potential (the B potential) were initially determined using the approximate electron-gas method.[14] Although these absolute energies may not be acceptable, differences between the potentials are considered to be useful. Since we have an acceptable Ce^{4+}-O^{2-} A potential, by taking the difference between the dopant-O^{2-} and electron gas B Ce^{4+}-O^{2-} potentials and adding this to the A Ce^{4+}-O^{2-} potential, an empiricized dopant-O^{2-} potential is obtained. The empiricized potentials are therefore consistent with the host lattice potentials. Discussions concerning the model parameters and the methodology generally can be found in recent reviews.[1,2,15]

III. RESULTS FOR CLUSTERS CONTAINING A SINGLE OXYGEN VACANCY

A. The formation of defect pairs

Explicitly, the binding energy BE of a defect cluster is equal to the sum of the defect energies of the cluster's component point defects, minus the defect energy of the cluster itself:

$$BE_{cluster} = \sum_{components} E_{defect} - E_{cluster}.$$

A positive binding energy therefore indicates a preference for the cluster over its components. However, with respect to a defect energy, a positive energy implies that energy is required to form the defect. As such, the defect or defect cluster with the lowest positive or highest negative energy is preferred.
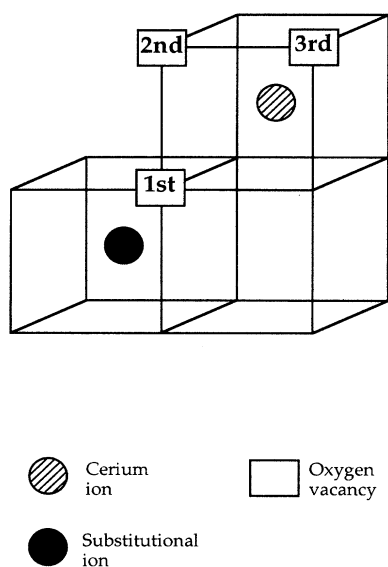
FIG. 1. First, second, and third neighbor oxygen ion lattice sites with respect to a substitutional ion at (000).

If Cd^{2+} or In^{3+} substitutional defects are to be present in CeO_2, charge-compensating oxygen vacancies will be required.[16] Indeed, the mechanism of forming the PAC parent In^{3+} defects from the oxide In_2O_3 can be considered as

$$In_2O_3 + 2Ce_{Ce}^X + 4O_O^X \rightarrow 2In_{Ce}' + 3O_O^X + V_O^{\cdot\cdot} + 2CeO_2 .$$
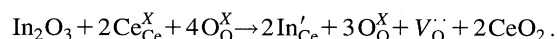
The cation defects and vacancy centers will Coulombically attract and form bound defect centers.

The defect clusters we shall consider consist of a Cd^{2+} or an In^{3+} ion substituting for a Ce^{4+} lattice ion, and an adjacent vacant O^{2-} lattice site. Figure 1 illustrates the locations of an oxygen vacancy in a first-, second-, and third-neighbor site with respect to the substitutional ion. The binding energies of an oxygen vacancy to a substitutional ion are given in Table III. In the case of the Cd^{2+} substitutional ion, the binding energy of the oxygen vacancy decreases as a function of the distance away from the substitutional site. Since the oxygen vacancy has an effective charge of $2+$ and the metal substitutional site a charge of $2-$, the position preference is clearly being dominated by the Coulombic attraction.

TABLE III. Binding energies (in eV) of a single oxygen vacancy to a substitutional ion.

Location of oxygen vacancy	Substitutional ion at [000]	
	Cd^{2+}	In^{3+}
First neighbor [111]	1.14	0.44
Second neighbor [113]	0.88	0.42
Third neighbor [133]	0.31	0.10

This interpretation is supported by the similarity of the eight coordinate ionic radius of Cd^{2+} (1.10 Å) compared with that of Ce^{4+} (0.97 Å).[17]

Conversely, in the case of the In^{3+} substitutional ion, the first- and second-neighbor sites for the oxygen vacancy exhibit essentially the same binding energy, although the third-neighbor site is decidedly less favorable. The equality of the first- and second-neighbor sites with respect to indium solution is due to a competition between Coulombic and relaxation energies. Clearly the Coulombic energy would favor the first-neighbor site over the second. This is supported by the predicted defect formation energies in which all the ions are constrained to their positions in the perfect CeO_2 lattice (i.e., no relaxation has been allowed): first neighbor 59.69 eV; second neighbor 65.13 eV. However, the energy gained when the ions are allowed to adopt positions of minimum energy, the relaxation energy, favors the second-neighbor site and this cancels this difference in Coulombic preference: the relaxation energy gained by the first-neighbor configuration is 11.26 eV; by the second neighbor, 16.64 eV. The most significant factor in promoting the greater second-neighbor relaxation energy is that the Ce^{4+} ion adjacent to the oxygen vacancy, in relaxing away from the vacant site (which is Coulombically desirable), is not forced to relax away from the site occupied by the In^{3+} ion. In the first-neighbor configuration, if the Ce^{4+} ion was to relax away from the oxygen vacancy, it would also force the Ce^{4+} ion away from the In^{3+} site which is energetically unfavorable. This relaxation effect should not be confused with a simple ion size effect. Indeed, the In^{3+} eight coordinate ionic radius, 0.92 Å, is very similar to that of Ce^{4+} (0.97 Å).[17]

B. Oxygen ion migration paths and activation energies

In this section we have calculated the energy to move an oxygen ion from its original site, through the lattice, to occupy an adjacent vacant oxygen site: that is, the activation energy for oxygen ion migration via an oxygen vacancy mechanism. The activation energy for such a migration is predicted to be the maximum value of the defect energy during the ion's migration, minus the defect energy of the initial configuration. The defect during the migration process therefore consists of an interstitial oxygen ion and two oxygen vacancies. The process is considered in an otherwise defect-free lattice and adjacent to a substitutional dopant ion.

Consider the set of planes whose normal is the vector connecting the initial and final locations of the oxygen vacancy (or, equivalently, the initial and final locations of the oxygen ion). The migrating oxygen ion must pass through each of these planes, and will do so at the point for which the resulting defect energy is a minimum. The maximum value of the defect energy experienced as the oxygen ion migrates was assumed to occur when it passed through the plane of maximum defect energy (but at the point of minimum defect energy within this plane). In practice, a representative series of planes was chosen and the locus of minimum energy points was fitted to a quadratic function whose maximum was determined. In all cases, one explicitly determined plane was close enough to the maximum to guarantee the accuracy to which the activation energies are reported.

TABLE IV. Oxygen ion migration activation energies (in eV) in undoped ceria. The figures in bold indicate the most energetically favorable mechanism for the specified migration. $\langle abc \rangle$ indicates the vector between the initial and final location of the oxygen ion, not its precise path.

Path of oxygen ion	Activation energy
$\langle 100 \rangle$	**0.74**
$\langle 110 \rangle$	3.66
$\langle 111 \rangle$	4.95

1. Undoped ceria

When there is no substitutional ion present, the increased symmetry reduces the number of unique migration paths. Those where the vector between the initial and final sites of the oxygen ion/vacancy is $\langle 100 \rangle$, $\langle 110 \rangle$ or $\langle 111 \rangle$ were investigated and their activation energies are shown in Table IV. The most direct $\langle 100 \rangle$ migration pathway is clearly the most favorable migration pathway. This predicted value for oxygen migration in pure CeO_2, via a vacancy mechanism is therefore 0.74 eV. This is in excellent agreement with the experimental value of 0.76 eV.[18]

2. Cadmium and indium doped ceria

The investigation of migration pathways for In-doped materials assumes the oxygen vacancy to be initially in either a first- or second-neighbor site with respect to the substitutional ion. Depending on the position of the vacancy, the oxygen ion may then either move 1st→1st (from a first-neighbor site to another first-neighbor site); 2nd→2nd; 1st→2nd; or 2nd→1st. In all cases, there will be a choice of migration direction, e.g., $\langle 100 \rangle$ or $\langle 110 \rangle$.

The results in Table V show that as with the undoped material, $\langle 100 \rangle$ migration pathways are clearly favored. Figure 2 illustrates these $\langle 100 \rangle$ migration paths along with their activation energies. From this, it can be seen that, in both cadmium- and indium-doped ceria, an oxygen ion may migrate between first-neighbor sites via the mechanism 1st→2nd→2nd→1st with an activation energy of ~0.65 eV.

TABLE V. Oxygen ion migration activation energies (in eV) in doped ceria. Significance of bold figures and $\langle abc \rangle$ explained in Table IV.

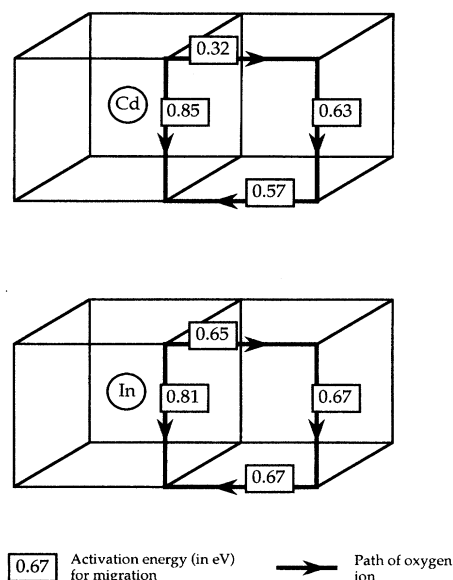| Path of oxygen ion | Substitutional ion (nonpol) | |
	Cd^{2+}	In^{3+}
1st→1st		
$\langle 100 \rangle$	**0.85**	**0.81**
$\langle 110 \rangle$	3.71	3.69
2nd→2nd		
$\langle 100 \rangle$	**0.63**	**0.67**
$\langle 110 \rangle$	4.03	4.05
1st→2nd		
$\langle 100 \rangle$	**0.32**	**0.65**
$\langle 111 \rangle$	4.25	4.63
2nd→1st		
$\langle 100 \rangle$	**0.57**	**0.67**
$\langle 111 \rangle$	4.47	4.64

FIG. 2. The most energetically favorable paths for the migration of oxygen ions, via oxygen vacancy mechanisms, in cadmium- and indium-doped ceria.

This value is in excellent agreement with the PAC derived value.[7] Interestingly, this is significantly lower than the activation energy for the direct 1st→1st mechanism. The results also suggest that the effective activation energy for an oxygen ion hopping, via a vacancy mechanism, around a cadmium or indium substitutional ion is lower than the activation energy for migration in undoped ceria albeit by a convoluted pathway.

IV. RESULTS FOR MORE COMPLEX DEFECT CLUSTERS

A. Defect clusters containing two oxygen vacancies

A defect cluster consisting of a substitutional ion and two nearby oxygen vacancies may be considered as a single oxygen vacancy defect cluster (described in Sec. III A), interacting with a second oxygen vacancy. If the first oxygen vacancy is assumed to be in a first-neighbor site, the second vacancy may be located in a first-, second- or third-neighbor site. These three possibilities are designated: 1st:1st; 1st:2nd; 1st:3rd. It is then possible to consider the situation where both oxygen vacancies are in second neighbor sites; 2nd:2nd. The respective cluster geometries are illustrated in Figs. 3 and 4. In all cases, there are a number of ways of placing the second vacancy in the lattice within the designation as defined. All the appropriate binding energies of the second oxygen vacancy to the substitutional ion:oxygen vacancy defect cluster are given in Table VI.

First let us consider clusters involving the Cd^{2+} ion. As might be expected on Coulombic grounds, the preferred position of the second vacancy within each of the designated classes is generally that which places the second vacancy as far away from the first vacancy as possible. However, the difference between the preference for the furthest and second furthest sites is generally minor. This leads to an exception to
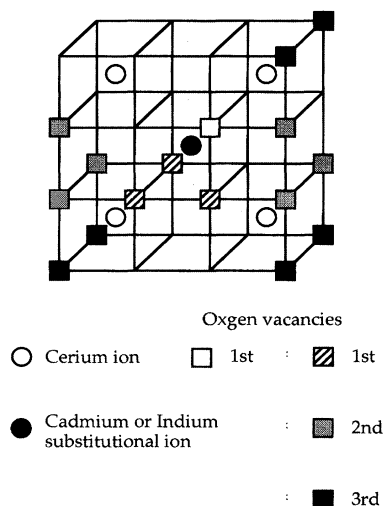
Oxgen vacancies

○ Cerium ion   □ 1st   ▨ 1st

● Cadmium or Indium
  substitutional ion   ▦ 2nd

                        ■ 3rd

FIG. 3. Unique defect cluster configurations for a substitutional ion (at [000]), and two oxygen vacancies whose locations are: 1st:1st; 1st:2nd; and 1st:3rd.

the "as far away" rule so that in the case of the 2nd:2nd cluster, there is a negligible preference for the [−1 1 −3] position rather than the further away [−1 −1 −3].

Even in the most favored positions, for all classes the binding energy of the second vacancy is substantially less than was the binding energy of the first vacancy to the substitutional ion. Clearly this would be expected due to the Coulombic repulsion between the vacancies. Nevertheless, the detailed situation is complicated. In particular, the binding energy of a second vacancy in a third-neighbor site when the first vacancy occupies a first-neighbor site is either unfavorable or practically zero in all cases.

Overall, the preference for the 1st:1st cluster in which the second vacancy occupies the highly symmetric
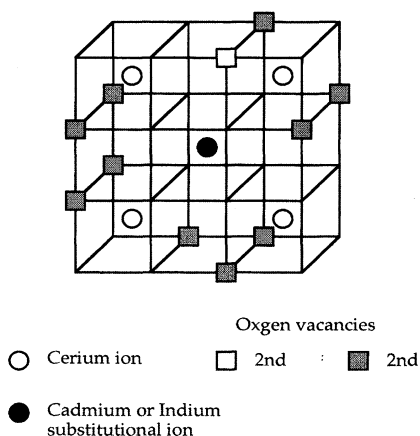

Oxgen vacancies

○ Cerium ion   □ 2nd   ▦ 2nd

● Cadmium or Indium
  substitutional ion

FIG. 4. Unique defect cluster configurations for a substitutional ion (at [000]) and two oxygen vacancies whose locations are 2nd:2nd.

TABLE VI. Binding energies (in eV) of a second oxygen vacancy to a pre-existing $\{M_{Ce}:V_O^{..}\}$ defect cluster; $M = Cd^{2+}$ or In^{3+}.

Locations of both oxygen vacancies	Substitutional ion at [0 0 0]	
	Cd^{2+}	In^{3+}
1st:1st		
[1 1 1]:[1 1 −1]	−0.27	−1.23
[1 −1 −1]	0.44	−0.45
[−1 −1 −1]	0.57	−0.25
1st:2nd		
[1 1 1]:[1 3 1]	−0.97	−1.37
[1 3 −1]	0.05	−0.49
[−1 3 −1]	0.15	−0.41
[1 −3 1]	0.15	−0.45
[1 −3 −1]ᵃ	0.39	−0.31
[−1 −3 −1]	0.43	−0.05
1st:3rd		
[1 1 1]:[1 3 3]	−0.57	−0.75
[−1 3 3]	−0.41	−0.58
[1 3 −3]ᵃ	−0.17	−0.39
[−1 3 −3]ᵃ	−0.19	−0.39
[1 −3 −3]	−0.07	−0.33
[−1 −3 −3]	−0.03	−0.28
2nd:2nd		
[1 1 3]:[1 −1 3]	−0.92	−1.37
[1 3 1]	−0.02	−0.49
[−1 3 1]	0.26	−0.27
[1 −3 1]ᵃ	0.49	−0.05
[−1 −3 1]ᵃ	0.46	−0.06
[1 −3 −1]	0.37	−0.12
[−1 −3 −1]	0.50	0.02
[1 1 −3]	0.30	−0.17
[−1 1 −3]	0.53	0.05
[−1 −1 −3]	0.46	−0.03

ᵃThese binding energies were determined using a region I size of $3.5a_0$ (9.47 Å) instead of $4.0a_0$ (10.82 Å), due to computational difficulties imposed by the particularly low symmetry of these defect configurations (see Sec. III B 1).

[−1 −1 −1] position is noteworthy. In addition, a number of significantly less symmetric arrangements are quite stable and only a little less preferred.

In the case of the In^{3+} clusters, the binding energies are negative or close to zero, indicating that at best, the second vacancy experiences no attraction to the In^{3+}:single vacancy di-cluster. This is not surprising given the overall negative charge of the In^{3+}:vacancy cluster. However, given the relative stability of a single vacancy to the second neighbor site, the results suggest that a second vacancy can reside at another second-neighbor site or perhaps even at a first-neighbor site with no energy penalty. In terms of relative preference, within a given class, a similar picture emerges for the In^{3+} clusters as for the Cd^{2+} clusters: the two oxygen vacancies will preferably be oriented as far from each other as possible.

B. Defect clusters containing two cation substitutional defects

Since larger clusters will be considered in this section, the number of possible arrangements of the defects is prohibi-

TABLE VII. Formation of clusters with two substitutional ions adjacent to an oxygen vacancy at (000): $\{In'_{Ce}:V_O^{\cdot\cdot}:In'_{Ce}\}$, $\{Cd''_{Ce}:V_O^{\cdot\cdot}:In'_{Ce}\}$ or $\{Cd''_{Ce}:V_O^{\cdot\cdot}:Cd''_{Ce}\}$.

Cluster	Position of In^{3+}	Total defect energy	Binding energy of second cation
$\{In^{3+}(111):V_O\}$	$(-1\ -1\ 1)$	80.88	0.20
$\{In^{3+}(111):V_O\}$	$(-3\ -1\ -1)$	80.76	0.33
$\{In^{3+}(311):V_O\}$	$(-1\ -1\ 1)$	80.76	0.33
$\{In^{3+}(311):V_O\}$	$(-3\ -1\ -1)$	80.76	0.32
	Position of Cd^{2+}		
$\{In^{3+}(111):V_O\}$	$(-1\ -1\ 1)$	107.36	0.76
$\{In^{3+}(111):V_O\}$	$(-3\ -1\ -1)$	107.41	0.71
$\{In^{3+}(311):V_O\}$	$(-1\ -1\ 1)$	107.14	1.00
$\{In^{3+}(311):V_O\}$	$(-3\ -1\ -1)$	107.45	0.69
	Position of In^{3+}		
$\{Cd^{2+}(111):V_O\}$	$(-1\ -1\ 1)$	107.36	0.00
$\{Cd^{2+}(111):V_O\}$	$(-3\ -1\ -1)$	107.14	0.23
$\{Cd^{2+}(311):V_O\}$	$(-1\ -1\ 1)$	107.41	0.22
$\{Cd^{2+}(311):V_O\}$	$(-3\ -1\ -1)$	107.45	0.18
	Position of Cd^{2+}		
$\{Cd^{2+}(111):V_O\}$	$(-1\ -1\ 1)$	133.94	0.49
$\{Cd^{2+}(111):V_O\}$	$(-3\ -1\ -1)$	133.82	0.61
$\{Cd^{2+}(311):V_O\}$	$(-1\ -1\ 1)$	133.82	0.61
$\{Cd^{2+}(311):V_O\}$	$(-3\ -1\ -1)$	134.25	0.18

tively large. As such, in all arrangements, unless otherwise stated, the defects of like charge are as far from each other, within the designated neighbor shell, as possible. This approach is justified on the basis of Coulombic repulsion and is supported by the results of Sec. IV A. The same approach will be taken in subsequent sections. With this in mind, the combinations of first- and second-neighbor cation sites with respect to an oxygen vacancy results in four arrangements (see Table VII).

Consider first the possible clusters that incorporate two In^{3+} defects. By comparing the total energies presented in Table VII, it is apparent that the situation in which both of the cations are in nearest-neighbor sites with respect to the oxygen vacancy is significantly less favorable compared with all other arrangements. All the other clusters are equally stable. Interestingly, the binding energy of the second In^{3+} ion to the $\{In'_{Ce}:V_O^{\cdot\cdot}\}$ cluster is 75% of that for the binding of an In^{3+} ion to the isolated oxygen vacancy (see Table III). The situation in which one of the In^{3+} ions is in a first-neighbor and the other in a second-neighbor site is shown in Fig. 5. At least part of the reason that the second-neighbor site is preferred for the second In^{3+} ion is a consequence of the fluorite structure. Cations in nearest-neighbor sites have one equal Cartesian coordinate, that is $[+1, +1, +1]$ and $[-1, -1, +1]$ and the cation-cation separation is rather close. If we compare coordinates of a first- and second-neighbor site; $[+1, +1, +1]$ and $[-1, -1, -3]$, it is clear that the cation-cation distance is substantially greater and the Coulombic repulsion between the defects is much reduced.

When both cations are Cd^{2+}, we find some preference for the second cation to occupy a second-neighbor site rather than a first-neighbor site given nearest-neighbor occupation by the first Cd^{2+} defect. As such, the most stable geometry

of the double Cd^{2+} cluster is identical to that for the double In^{3+} cluster. The binding energy of the second Cd^{2+} defect is favorable to the stability of this charged cluster.

If a mixed cluster is formed, that is, composed of one Cd^{2+} and one In^{3+} defect bound to an oxygen vacancy, the preference is for the Cd^{2+} ion to be in a nearest-neighbor site and for the In^{3+} ion to occupy the second-neighbor site (see Table VII). In other words, the geometry preference expressed by the single cation clusters is strongly reflected in the double cation clusters.

C. Defect clusters that incorporate small polarons

It has been established that electron conduction in CeO_2 proceeds via a localized small polaron hopping mechanism.[18,19] A polaron, in the context of our description of CeO_2, is therefore modeled as a Ce^{3+} ion. It is also well known that CeO_2 exhibits a broad, oxygen deficient range of
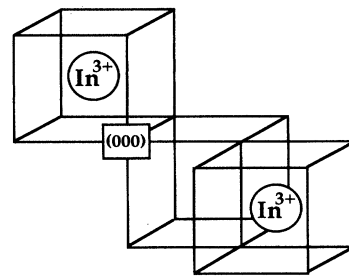
FIG. 5. Example of a neutral di-In^{3+}:oxygen vacancy cluster, $\{In^{3+}(111):V_O(000):In^{3+}(-3\ -1\ -1)\}$.

TABLE VIII. Binding energies (eV) of polarons (Ce^{3+}) to an isolated oxygen vacancy at (000) to form $\{Ce'_{Ce}:V_O^{..}\}$ or $\{Ce'_{Ce}:V_O^{..}:Ce'_{Ce}\}$ clusters.

Cluster	Position of Ce^{3+}	Total defect energy	Polaron binding energy
V_O	[111]	52.58	0.36
V_O	[311]	52.50	0.43
$\{Ce^{3+}[111]:V_O\}$	[$-1-1\ 1$]	89.30	0.20
$\{Ce^{3+}[111]:V_O\}$	[$-3-1\ 1$]	89.03	0.47
$\{Ce^{3+}[311]:V_O\}$	[$-1-1-1$]	89.03	0.40
$\{Ce^{3+}[311]:V_O\}$	[$-3-1\ 1$]	89.05	0.38

nonstoichiometry, CeO_{2-x}, where $x \leq 0.28$.[18] Indeed, there is some debate as to whether it is possible to form truly stoichiometric CeO_2. As such, in this section we shall consider the energetics of polaron binding to oxygen vacancies and their associated Cd^{2+} and In^{3+} substitutional ions.

1. Undoped ceria

In Table VIII we report the binding energies that describe the energetics of small polaron trapping by oxygen vacancies. The origin in this case is taken to be coincident with the oxygen vacancy. Two trap sites are considered for the polaron. The resulting cluster geometries are equivalent to the first- and second-neighbor clusters considered for the oxygen vacancy adjacent to the dopant ions in Sec. III A (and shown in Fig. 1). Analogous to the situation for the In^{3+} ion, the two trap sites for the polaron have similar energies. In fact, the preference for the second-neighbor site is slightly greater in the present case.

Tuller and Nowick[19] determined the difference between the formation enthalpies of a doubly charged and singly charged oxygen vacancy to be 0.56 eV. In our model this corresponds to the binding energy of a single polaron to an isolated oxygen vacancy. The calculations (see Table VIII) are therefore in good accord with experiment.

If two polarons are chosen, the combinations of first- and second-neighbor sites results in four arrangements as in Sec. IV B. The results of Table VIII show a similar situation energetically as was found for the double In^{3+}, oxygen vacancy defect clusters in Table VII. For example, by comparing the total energies in Table VIII, we find that the geometry in which both of the polarons are in nearest-neighbor sites with respect to the oxygen vacancy is significantly less favorable compared to all other arrangements. All the other clusters are equally stable. Geometries such as that shown in Fig. 5 are therefore expected.

The surprising result for the two polaron clusters is that the binding energy that the second polaron experiences to the

single polaron $\{Ce'_{Ce}:V_O^{..}\}$ cluster, ~0.4 eV, is as great as the binding energy of the first polaron to the isolated oxygen vacancy. Less surprising, given the Coulombic parity, is that the predicted binding energy of a polaron to an oxygen vacancy is very similar to that for an oxygen vacancy to an In^{3+} dopant ion (see Table III).

2. Binding of a polaron to a $\{M_{Ce}:V_O\}$ cluster

The results (see Table IX) when the substitutional ion is In^{3+} mirror those concerning the trapping of two polarons to an oxygen vacancy (see Table VIII and Sec. IV C 1). Thus, the arrangement when both the In^{3+} and Ce^{3+} ions are in nearest-neighbor sites with respect to the oxygen vacancy is significantly less favorable than the other three clusters.

If the substitutional ion is Cd^{2+}, the $\{M_{Ce}:V_O^{..}\}$ cluster is neutral. However, the binding energy for the polaron to this cluster is not predicted to be appreciably smaller than the case for the singly charged $\{In'_{Ce}:V_O^{..}\}$ cluster. (An exception is the case of the double nearest-neighbor cluster which, since it is highly unfavorable, should not be observed anyway.)

3. Binding of a polaron to a $\{V_O^{..}:M_{Ce}:V_O^{..}\}$ cluster

In Sec. IV C 1 the possibility of forming clusters with two oxygen vacancies was investigated. Here we considered how strongly trapped a polaron might be to such a cluster.

The results in Table X suggest that if the cation is In^{3+}, the double oxygen vacancy cluster will strongly trap a polaron. Indeed, the trapping energy of the polaron to the most stable double vacancy, 0.57 eV, is higher than that to a single oxygen vacancy, 0.44 eV (see Table III). The most stable trap site is, once again, at a second-neighbor site unless the In^{3+} cation is already in a second-neighbor trap site with respect to the oxygen vacancy in which case there is no energy penalty for the polaron to be in a first-neighbor site.

If the cation is Cd^{2+}, the double oxygen vacancy cluster will also strongly trap a polaron. The trapping energies in

TABLE IX. Binding energies (eV) of a polaron to a $\{M_{Ce}:V_O\}$ cluster; $M = Cd^{2+}$ or In^{3+}.

Cluster	Position of polaron	Total defect energy Cd	Total defect energy In	Polaron binding energy Cd	Polaron binding energy In
$M[111]:V_O$	[$-1-1\ 1$]	111.54	85.08	0.07	0.21
$M[111]:V_O$	[$-3-1-1$]	111.22	84.86	0.40	0.43
$M[311]:V_O$	[$-1-1\ 1$]	111.54	84.94	0.35	0.35
$M[311]:V_O$	[$-3-1-1$]	111.60	84.90	0.29	0.39

TABLE X. Formation of $\{Ce'_{Ce}:V_O^{\cdot\cdot}:M_{Ce}:V_O^{\cdot\cdot}\}$ clusters; $M = Cd^{2+}$ or In^{3+}. All energies in eV.

Cluster	Position of polaron	Total defect cluster energy		Binding energy of polaron to $\{V_O^{\cdot\cdot}:M_{Ce}:V_O^{\cdot\cdot}\}$ cluster		Binding energy with respect to $\{M_{Ce}:V_O^{\cdot\cdot}\}$ and $\{Ce'_{Ce}:V_O^{\cdot\cdot}\}$ clusters	
		Cd	In	Cd	In	Cd	In
$\{V_O:M_{Ce}[111]:V_O[222]\}$	$[-1\ -1\ 1]$	126.97	101.32	0.27	0.39	0.29	-0.38
$\{V_O:M_{Ce}[111]:V_O[222]\}$	$[-3\ -1\ -1]$	126.69	101.14	0.55	0.57	0.49	-0.27
$\{V_O:M_{Ce}[311]:V_O[422]\}$	$[-1\ -1\ 1]$	127.28	101.29	0.47	0.49	-0.03	-0.35
$\{V_O:M_{Ce}[311]:V_O[422]\}$	$[-3\ -1\ -1]$	127.34	101.27	0.42	0.52	-0.15	-0.40
$\{V_O:M_{Ce}[311]:V_O[622]\}$	$[-1\ -1\ 1]$	127.74	101.66	0.43	0.45	-0.21	-0.72
$\{V_O:M_{Ce}[311]:V_O[622]\}$	$[-3\ -1\ -1]$	128.13	101.96	0.04	0.15	-0.67	-1.09

these cases are only slightly lower than for the In^{3+} containing clusters. Again, the favored trap site for the polaron is a second-neighbor site as shown in Fig. 6.

4. Binding of a $\{M_{Ce}:V_O^{\cdot\cdot}\}$ cluster to a $\{Ce'_{Ce}:V_O^{\cdot\cdot}\}$ cluster

The large defect clusters considered in the last section can be constructed from smaller pairs of defects. In Table X, the binding energies of such clusters, when the cation is In^{3+}, show the larger cluster aggregate to be markedly unstable with respect to decomposition to the smaller stable defect pairs. That is, the binding of a polaron to the double cluster actually makes the cluster unstable and prone to dissociation. This is despite the fact that in the most stable configurations the nonpolaron compensated double oxygen vacancy showed little preference to dissociate (see Table VI). If the cation is Cd^{2+}, the most stable two configurations are also stable with respect to aggregation.

V. SUMMARY

The simulations suggest that in general, the Cd^{2+} ion prefers to be in a nearest-neighbor site with respect to an oxygen vacancy. However, for In^{3+} the situation is more complex. If only one In^{3+} ion is involved, the In^{3+} ion exhibits an equal predisposition for the first- and second-neighbor site. Upon the association of a second In^{3+} ion, the preference is clearly for a second-neighbor site. For clusters involving polarons, the Ce^{3+} ion acts rather similarly to the In^{3+} ion often preferring the ubiquitous second-neighbor site.

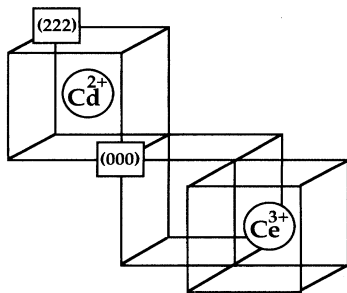Clusters involving two oxygen vacancies will form if the

FIG. 6. The most stable arrangement of the $\{Ce^{3+}(-3-11):V_O(000):Cd^{2+}(111):V_O(222)\}$ defect cluster.

associated cation is Cd^{2+} but are unstable or at best show zero binding energy for the second vacancy if the cation is In^{3+}. If polaron defects are available to the double oxygen vacancy they will bind strongly in all cases. However, if the substitutional defect is In^{3+}, the associated polaron will cause the $\{V_O^{\cdot\cdot}:In'_{Ce}:V_O^{\cdot\cdot}:Ce'_{Ce}\}$ cluster to become unstable with respect to smaller defect pairs.

The oxygen ion migration pathways also show a surprising behavior. For both substitutional ions, the lowest migration route, via a vacancy mechanism, involves the second-neighbor site.

One of the most important features of this work is the synergy between the results of computer simulation and those of experiment. The experimental results provide a quantitative verification of certain of the simulation predictions and hence justify the choice of technique and parameters employed.

The simulations also provide an atomistic interpretation of the observations—that, for samples with modest vacancy concentrations, all the ^{111}Cd ions have a trapped first-neighbor oxygen vacancy above 150 °C but that at low temperatures only about half of these daughter ions have such a first-neighbor oxygen vacancy. Below $\sim$100 °C half have trapped first-neighbor vacancies and half trap an electronic hole and have a characteristic "aftereffects" feature in the PAC spectra.

Wang et al.[6] noted that these observations follow from the energy computations and the reasonable assumption that a first-neighbor vacancy to Cd prevents hole trapping and consequently suppresses aftereffects. The energy calculations imply that the fraction of first- and second-neighbor indium/vacancy pairs is comparable but that when ^{111}In decays to Cd, the second neighbors should largely jump to first-neighbor positions. The energy barrier makes this too slow at low temperatures to effect PAC, but at some temperature (in this case between 100 and 150 °C) the jump becomes fast enough to free the trapped hole and result in a first-neighbor PAC spectrum for all probes. Wang et al. estimated that the jump barrier between the second- and first-neighbor vacancy trap position to Cd was of the order 0.4–0.5 eV, close to the calculated value of 0.32 eV (see Table V and Fig. 2).

Calculations concerning the more complex defect clusters have also provide important insight that has enabled us to better understand some of the experimental results. For example, with respect to Sec. IV, there is clear evidence, obtained by PAC on ceria doped with very dilute concentrations of radioactive ^{111}In probe atoms, that two oxygen vacancies

bind to a single indium dopant.[5,6] When samples are doped with yttrium or are depleted of oxygen by heating in vacuum sufficiently to increase the oxygen vacancy concentration to $\sim 0.05\%$, a significant fraction of the ^{111}In PAC probe atoms bind to two oxygen vacancies. At least two double vacancy configurations exist, one having both vacancies in symmetric first-neighbor positions on opposite sides of the indium atom, and one in which two vacancies are trapped in nonsymmetric positions.

Although the PAC technique cannot determine the charge state of a defect cluster directly, the experimental data does indicate that the symmetric configuration of the $\{V_O^{\cdot\cdot} : In_{Ce}' : V_O^{\cdot\cdot}\}$ cluster does trap one or more polarons and that the nonsymmetric configuration traps fewer polarons. Section IV A implies that both these configurations must include polarons otherwise the second vacancy would be un-

bound. The experiments in turn imply that there are stable complexes consisting of a single indium, two oxygen vacancies and polarons. We expect further coordinated experimental and computational research to provide a much better understanding of defects and defect complexes in ceria and related oxides.

[*]Author to whom correspondence should be addressed. Correspondence address: Department of Materials, Imperial College, Prince Consort Road, London SW7 2BP.

[†]Present address: Catalytica Inc., Mountain View, California.

[1] Computer simulation of defects in polar solids; special issue of J. Chem. Soc. Faraday Trans. **85**, No. 5 (1989). Guest editors are C. R. A. Catlow and A. M. Stoneham.

[2] C. R. A. Catlow and W. C. Mackrodt, in *Computer Simulation of Solids*, edited by C. R. A. Catlow and W. C. Mackrodt (Springer-Verlag, Berlin, 1982).

[3] H.-T. Su, R. Wang, H. Fuchs, J. A. Gardner, W. E. Evenson, and J. A. Sommers, J. Am. Ceram. Soc. **73**, 3215 (1990).

[4] R. Wang, J. A. Gardner, W. E. Evenson, and J. A. Sommers, in *Point Defects and Related Properties of Ceramics*, Ceramic Transactions Vol. 24, edited by T. O. Mason and J. L. Routbort (American Ceramic Society, Westerville, OH, 1991).

[5] R. Wang, J. A. Gardner, W. E. Evenson, and J. A. Sommers, in *Proceedings of the XII International Conference on Defects in Insulating Materials*, edited by O. Kanert and J.-M. Spaeth (World Scientific, Singapore, 1993), Vol. 2.

[6] R. Wang, J. A. Gardner, W. E. Evenson, and J. A. Sommers, Phys. Rev. B **47**, 638 (1993).

[7] H. Guan, Ph.D. thesis, Brigham Young University, 1994.

[8] M. Leslie (unpublished).

[9] B. G. Dick and A. W. Overhauser, Phys. Rev. B **112**, 90 (1958).

[10] V. Butler, C. R. A. Catlow, B. E. F. Fender, and J. H. Harding, Solid State Ionics **8**, 109 (1983).

[11] A. N. Cormack, C. R. A. Catlow, and A. S. Nowick, J. Phys. Chem. Solids **50**, 177 (1989).

[12] T. X. T. Sayle, S. C. Parker, and C. R. A. Catlow, J. Chem. Soc. Chem. Commun. 977, (1992).

[13] R. W. Grimes, C. R. A. Catlow, and A. M. Stoneham, J. Phys. Condens. Matter **1**, 7367 (1989).

[14] J. H. Harding and A. H. Harker, UKAEA Harwell Report No. R-10425. United Kingdom Atomic Energy Authority, Harwell, UK, 1982.

[15] *The Practical Calculation of Interionic Potentials in Solids*, edited by A. H. Harker and R. W. Grimes [Mol. Simul. 4, No. 5 (1996); **5**, No. 2 (1996)].

[16] D. J. M. Bevan and J. Kordis, J. Inorg. Nucl. Chem. **26**, 1509 (1964).

[17] R. D. Shannon, Acta Crystallogr. **A32**, 751 (1976).

[18] H. L. Tuller and A. S. Nowick, J. Electrochem. Soc. **122**, 255 (1975).

[19] H. L. Tuller and A. S. Nowick, J. Phys. Chem. Solids **38**, 859 (1977).